# Seismic Monitoring of Reinforced Concrete Buildings Following the Mw 8.8 Feb 27th, 2010 Offshore Maule Earthquake in Chile


**A. Lemnitzer**
*Assistant Professor, University of California, Irvine, USA*

**D. A. Skolnik**
*Senior Engineer, Kinemetrics Inc., Pasadena, CA, USA*

**L. Massone**
*Assistant Professor, University of Chile, Santiago, Chile*

**J.C. de la Lerra**
*Dean, Pontificia Universidad Cathólica de Chile, Santiago, Chile*

**J. W. Wallace**
*Professor, University of California, Los Angeles, USA*

**SUMMARY**

Following the February 27, 2010 Mw 8.8 earthquake impacting central Chile, a team of U.S. researchers, professionals, and local collaborators instrumented several reinforced concrete buildings in Santiago, Chile, to measure aftershock response data. The selected buildings, designed according to ACI 318-95, represent typical construction, e.g. moderate to high rise office buildings with large office space and inner core shear walls and mid-rise residential shear wall buildings. Instrumentation consisted mainly of accelerometers as well as some displacement transducers with data recorded using digitizers. Several aftershocks were captured over a period of one month. Data collected were processed and system identification algorithms were used to determine modeling parameters (e.g. building periods, acceleration amplification, inter-story drifts). Investigations included analyses to assess building rocking and torsion, and assessment of diaphragm in-plane rigidity. An overview of the instrumented buildings, recorded data, and analytical results will be presented, as well as practical lessons and limitations associated with monitoring studies conducted in foreign countries.

*Keywords: seismic monitoring, reinforced concrete structures*

## 1. INTRODUCTION

Building instrumentation in seismically active areas has become increasingly important to gain insight into building behaviour under earthquake loading. While permanent instrumentation programs are gaining traction throughout the globe, their evolution is slow due to high expenses associated with equipment installation and maintenance. Temporary instrumentation programs in areas with recent seismic events provide a unique opportunity to collect a significant amount of data over a short period of time. Furthermore, aftershock studies offer excellent opportunities to capture unique data when buildings damaged in the main shock are targeted.

Several hundred aftershocks followed the Magnitude 8.8 earthquake on February 27th 2010 near Conception, Chile and offered the opportunity to record structural aftershock response data. Most large magnitude shocks (M>6.0) occurred within 24 hours after the main shock (EERI 2010), while moderate aftershocks continued for over 5 weeks following the main shock. The epicenters of most aftershocks were located near the epicenter of the Mw 8.8 earthquake (i.e. near Concepcion), but were still felt in circumferences of up to 600 km, including the areas of Vina del Mar, Santiago and Mendoza. A team of academics and professionals visited several reinforced concrete buildings in Santiago as part of a reconnaissance effort in March 2010 and selected 4 buildings for temporary instrumentation over a period of 4 – 8 weeks. The buildings were chosen based on their availability and design similarities to US reinforced concrete structures to make measured data most beneficial for

both countries. The selected structures were designed using the current local building code, which can be compared to the ACI 318-95 specifications in the United States. Several initiatives on code revisions based on structural performance during the $M_w$ 8.8 earthquake are currently underway in Chile.

The objective of this study was to collect structural performance data that would enable system identification analyses and provide building modelling parameters such as periods and damping, acceleration amplification factors, inter-story drifts, and rocking and torsion effects to guide subsequent modelling studies. This study also forms an initiative to create a unique database of structural input and response data from aftershocks and main shocks. All data of this instrumentation effort are publicly available at the NEES project warehouse which can be found at http://nees.org/warehouse.

## 2. SELECTED CASE STUDIES & INSTRUMENTATION

Two of the four instrumented buildings were selected for presentation in this paper. "*Building A*" (shown in Figure 2.1a) is a 10 story reinforced concrete building with six levels of subterranean parking and is located in Santiago's business district "Las Condes" in the North-East of the city. The building was still under interior construction at the point of instrumentation and provided several unoccupied floors for easy access and installation. The structural system consisted of small inner core shear walls formed by the elevator shaft and an external beam- column framing system. The office building is a representation of a structure in the Occupancy Category 2 (IBC, 2010).The building did not suffer any structural damage during the $M_w$ 8.8 earthquake or its subsequent aftershocks.

The second building, referred to hereafter as "*Building B*", was located in a newly developed residential district of Santiago in the north east of the city (Independencia) and represents a 10-story reinforced concrete shear wall building with one level of underground parking. At the time of instrumentation only floor 2 and 9 were unoccupied and chosen for instrumentation. The building suffered structural damage at the underground parking level which consisted mainly of concrete cracking and rebar buckling at the column and wall – ceiling slab connections. Damage on the ground level included column buckling in 2 structural columns supporting the second floor, and moderate cracks along interior and exterior shear walls. Smaller shear cracks were also observed in floors 2-10, mostly occurring in exterior walls when windows were present in the walls on the floors below. Figure 2.1c shows an outside view of *Building B* and Figure 2.2 a-d presents photographs of some structural damage observed in *Building B*.

**Figure 2.1 a,b&c:** Photographs of instrumented *Building A* (2 left photographs) & *B* (right) in Santiago

The majority of the instrumentation in *Buildings A* and *B* consisted of uniaxial and triaxial Episensor accelerometers with a measurement range of ± 4 g. Additionally, several linear voltage differential transducers (LVDTs) were used for monitoring displacements of a reinforced concrete shear wall in *Building B*. All data were recorded with Quanterra Q330 digitizers and processed with MATLAB (2010). Data were recorded at a sampling rate of 200 sps, and recording was triggered when accelerometer readings exceeded a threshold of 0.05g. Each event included 15 seconds of pre- and

post-event data. The monitoring system was powered using 12V Car batteries which were locally purchased and charged onsite. All monitoring equipment are property of the NEES@UCLA equipment site and were imported into the country from the US using a temporary instrumentation permit issued by the customs and immigration office upon arrival in Santiago.

**Figure 2.2 a-d(left to right):** Structural damage in building 2. From left to right: (a&b) column damage on the ground level floor, (c) wall damage at the underground parking levels, (d) Shear wall damage at ground level

In *Building A*, a total of eight accelerometers were installed. Four accelerometers were placed on the first and 10th floor levels at all 4 corners. Figure 2.3a shows a schematic of the floor plan and the sensor layout. The footprint of *Building A* is approximately 3209 m². All instrumentation was directly mounted on the reinforced concrete slabs. Both floors were completely unoccupied and in its raw interior construction stage (see Figure 2.1b). Four aftershocks along with large amounts of ambient vibrations were measured in *Building A*.

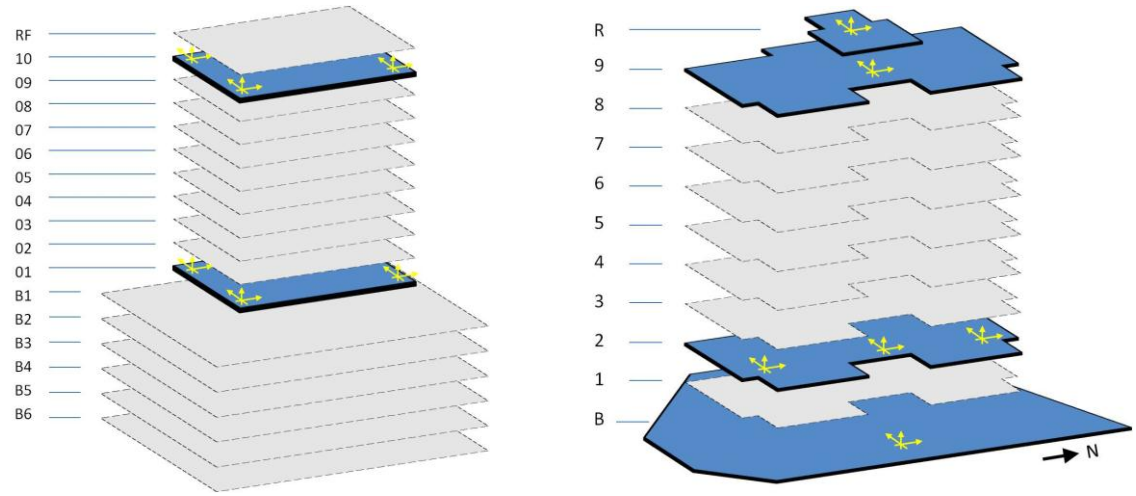


**Figure 2.3 a&b.** Model of Building A (left) & B (right) and location of sensor installation

*Building B* was instrumented with one accelerometer at the center of the building on the basement slab (i.e. on the concrete slab at underground parking level), three triaxial accelerometers on the second floor (installed on tile floors, or directly on concrete slab), one accelerometer at the ninth floor (on concrete slab) and three uniaxial accelerometers at the roof (installed at the concrete slab). A layout of the floor plan with the instrumentation is illustrated in Figure 2.3b. A total of 30 aftershocks were recorded between March 18th to May 5th 2010 in *Building B* with peak ground accelerations ranging from 0.5cm/s$^2$ to 7 cm/s$^2$ (0.05 to 0.7%)g. A total of 22 aftershocks were used for the proceeding data evaluation and analysis.

## 3. AFTERSHOCK MEASUREMENTS

### 3.1. Building A

The building response of *Building A* is presented via data recorded during an aftershock on March 25, 2010 at 10:59:35 am local time (12:59:35 pm UTC time). According to the Seismic Network of Chile (*http://ssn.dgf.uchile.cl/seismo.html*), the aftershock measured a magnitude of M4.7 and its epicenter was located about 17km north of Pichilemu (~ 200 km from Santiago) at a depth of 34.5 km.
Prepossessing of the recorded structural accelerations included filtering with linearbandpass filters and baseline corrections . Several different sets of measured accelerations at the corners were used to calculate the three dimensional (two translational and torsional) slab motions at a central point assuming that each slab behaves as a rigid diaphragm. Results showed that the rigid diaphragm assumption is sound and max values of 1.2cm/s$^2$ both, in EW and NS directions were found. No torsion was measured on floor one. Accelerations for the same aftershock on floor 10 measured center accelerations of 3.5 cm/s$^2$ and corner accelerations of 4.5 cm/sec$^2$ in the EW direction, and center accelerations of 2.8 cm/s$^2$ and corner accelerations of 5.0 cm/sec$^2$ in the NS direction. The amplification of acceleration between floor one and ten is in the range of 2.0 – 4.5 (center and corner respectively). Torsion was observed on the 10th floor and is shown along with story accelerations in Figure 3.1.

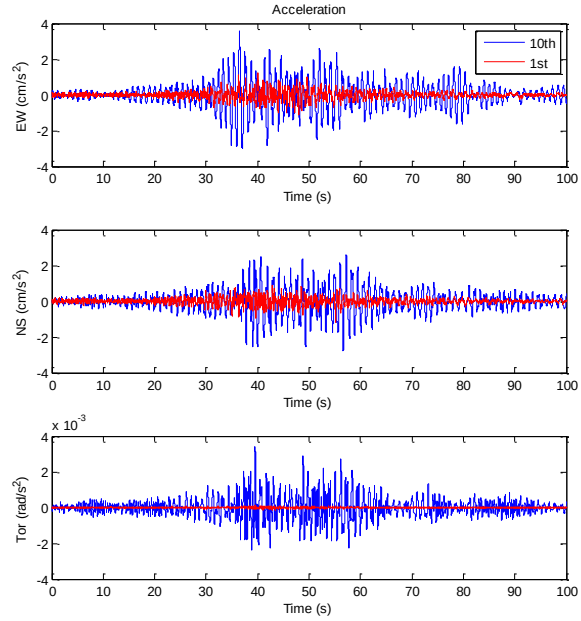


**Figure 3. 1.** Acceleration-Time Histories for *Bldg. A*

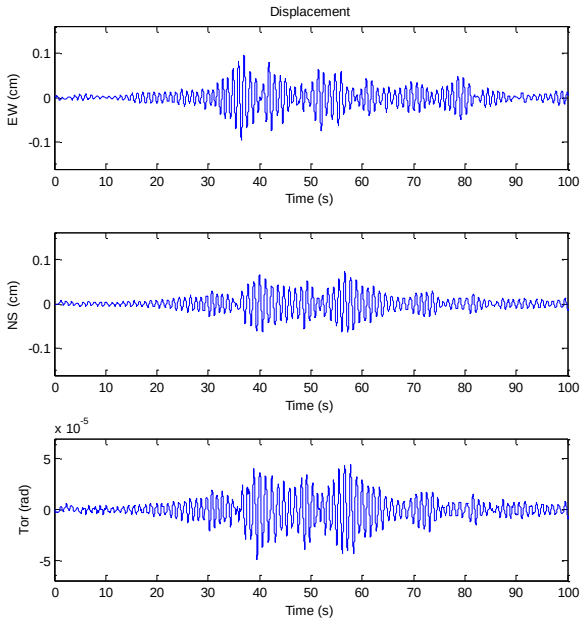


**Figure 3. 2.** Displacement-Time Histories for *Bldg. A*

Double integration of recorded accelerations enabled calculations of story displacements. In the E-W direction, a maximum displacement of 0.0167 cm and 0.1042 cm was measured for floors one and ten, respectively. The inter-story drift between both floors was 0.0875 cm. In the N-S direction, maximum displacements of 0.0147 cm and 0.0609 cm were recorded for floor one and ten respectively, resulting into an inter story drift of 0.0462, which is approximately half of the drift measured in the orthogonal direction. Displacement measurements confirm no torsion at level one, but twisting on floor 10. Story displacements in E-W, N-S and torsional direction are shown as relative displacements in Figure 3.2, therefore only displacement –time histories for floor 10 is presented.
The maximum torsional acceleration on the first and tenth floor is 1.273x10$^{-4}$ rad/s$^2$ and 3.386x10$^{-3}$ rad/s$^2$ and the maximum torsional displacement on the first and tenth floor is 5.56x10$^{-7}$ rad and 4.56x10$^{-5}$ rad, respectively.
The XY displacement of the center of floor ten is shown as particle motion – time history for the duration of the aftershock in Figure 3.3. The observed amplification is uniform and confirms previous results on torsional movement of the slab.
Fast Fourier Transforms (FFT) were computed to estimate the buildings natural frequencies. From Figure 3.5, it can be seen that the first natural frequency is evident in both directions (EW and NS) as well as in the torsional measurements. A possible second mode of the structure is only evident in the NS direction. Transfer functions were developed for E-W, N-S and torsional direction to accurately identify the seismic parameters of the first and second building mode (Figure 3.4). The maximum

Fourier amplitude occurred at a frequency of 0.96 Hz representing the building's natural frequency in the E-W direction. The corresponding natural E-W building period was calculated to be 1.04s. For this direction, no second mode frequency was observed – which is consistent with results presented in Figure 3.5. In the N-S direction, maximum Fourier amplitude occurred at a frequency of 0.91 Hz and had a period of 1.1 s in the first mode. A second natural frequency may be identified for the N-S direction at about 2.35 Hz, corresponding to a 2nd mode period of 0.42 sec, which is consistent with tenth floor FFT functions shown in Figure 3.5. The torsional natural frequency had a maximum Fourier amplitude at 0.89 Hz (T=1.1sec).

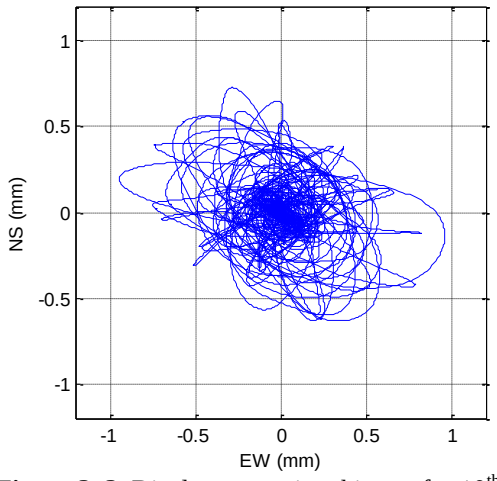


**Figure 3. 3.** Displacement-time history for 10th floor particle motion at the center

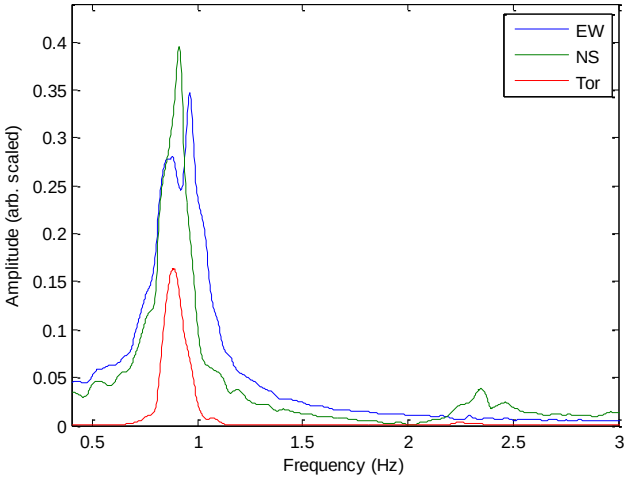


**Figure 3. 4.** Transfer functions for *Building A*

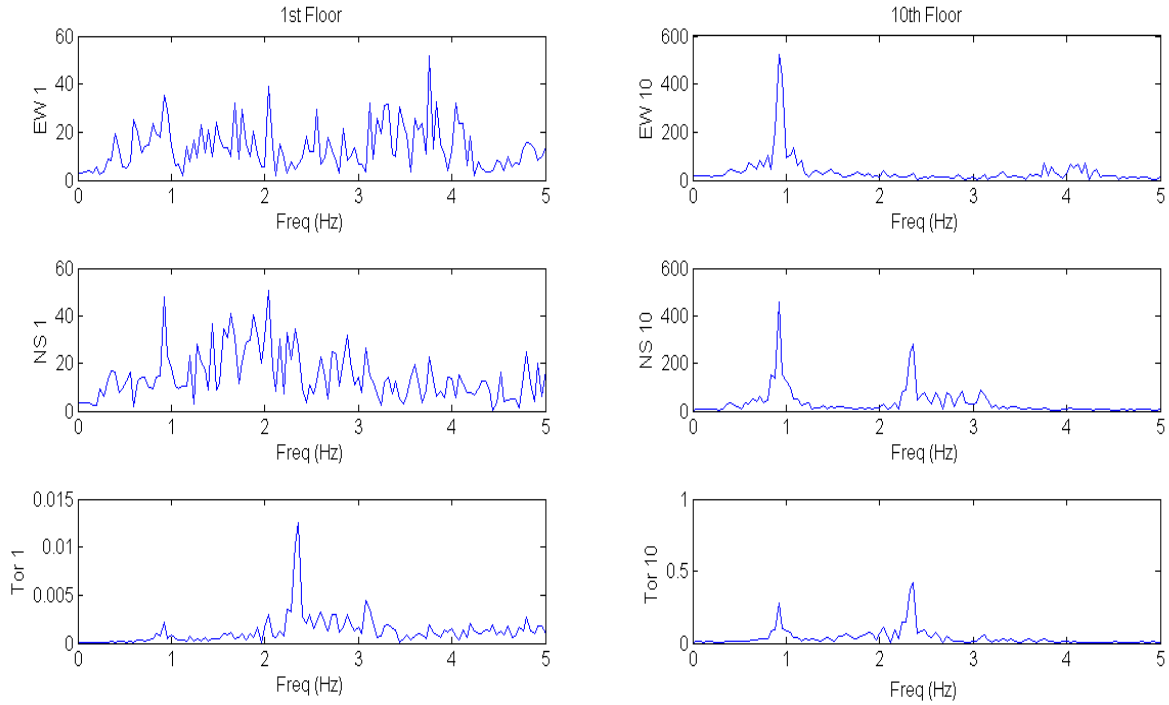


**Figure 3. 5.** Fast Fourier Transform Functions for *Building A*

### 3.2. Building B

A 5.8 Magnitude aftershock which occurred on May 2nd, 2010 at10:52:30 local time (14:52:39 UTC) at a depth of 32.9 km, 12 km north of Pichilemu (see Figure 3.6, *http://ssn.dgf.uchile.cl/seismo.html*) was identified as the strongest aftershock in terms of absolute accelerations, and selected for detailed processing in *Building B.*

The peak ground accelerations (PGA) reached about 6.1 cm/ sec$^2$ (0.6% g).

The structural accelerations measured in the building are presented in Figure 3.7. Again, band-pass filtering that ranged between 0.1 and 25Hz was implemented for data preprocessing. Second floor accelerations were estimated using a least square analysis since the three triaxial sensors installed at that level (see Figure 2.3b), over-determined the assumed 3 translational DOF of the floor (x, y and z). Maximum 2nd floor accelerations of 6.6 cm/sec$^2$ (0.7%g) and 11.2 cm/sec$^2$ (1.1%g) were measured in EW and NS directions respectively. Ninth floor structural accelerations measures 8.7 cm/sec$^2$ (0.9%g) and 13.4 cm/sec$^2$ (1.4%g) in the EW and NS direction, respectively and maximum roof accelerations increased to 21.4 cm/sec$^2$ (2.2%g) and 20.6 cm/sec$^2$ (2.1%g) in EW and NS direction, respectively. The amplification of accelerations from ground to roof was calculated to be 5.3 in the EW direction. For the NS direction a total amplification of accelerations of 3.4 between ground floor and roof.

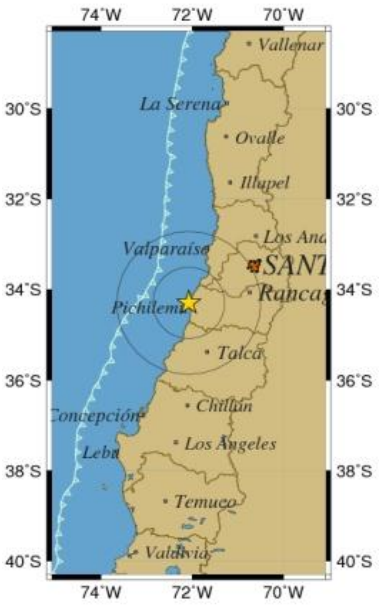


**Figure 3. 6.** Map of aftershock on March 25th, 2010

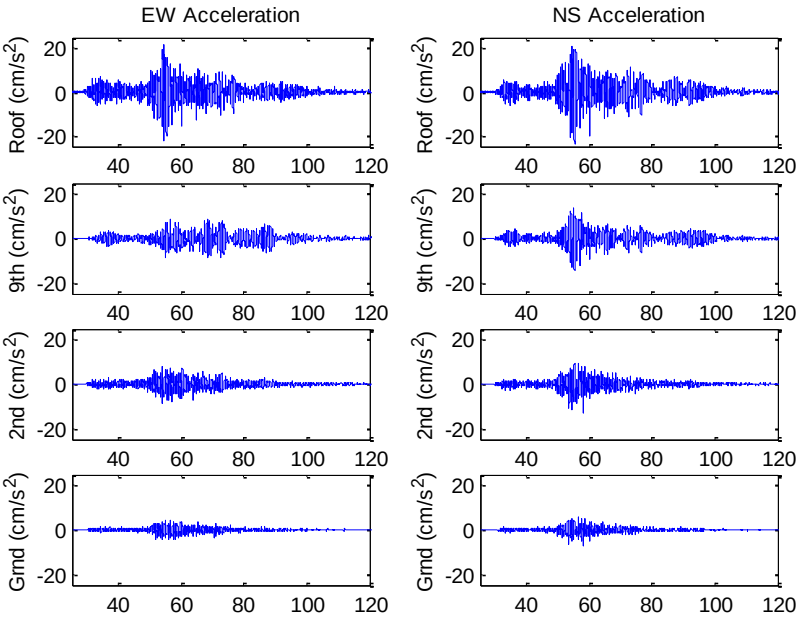


**Figure 3. 7.** Story accelerations in EW and NS direction in Building B

Given the instrumentation configuration on the 2nd floor, torsional and translational accelerations could be determined and are shown in Figure 3.8. The maximum torsional acceleration reaches about 0.004 rad/s$^2$. Torsional accelerations were determined in a similar fashion as described for *Building A* and least square fitting was implemented to reduce the overdetermined system at that level. The largest translational acceleration measurement in floor 2 reached about 10 cm/sec$^2$ (1%g) in both NS and EW direction. Thus, a sensor located 10 m away from the central sensor would result in an increment of translational acceleration of 4cm/sec$^2$ (0.004*1000) due to torsion, which corresponds to about 40% of the translation of the central sensor, indicating that the torsional component has a significant impact in the response in *Building B.*

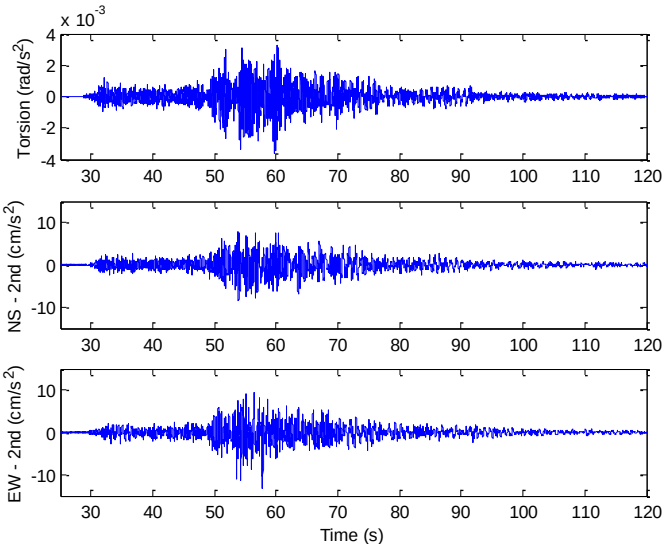


**Figure 3. 8.** Translational and torsional accelerations in the 2nd floor

Figure 3.9 shows the EW and NS absolute displacements components of all instrumented floors. The displacements were determined by double-integrating the accelerations of each level and applying a high-pass filter for 0.2 Hz to overcome residual displacements. The peak ground displacement reaches about 0.08 cm in the NS direction and about 0.04 cm in the EW direction. Maximum displacements at the second floor reached values of 0.11 cm in NS and xx 0.06 cm EW direction. Displacements increased at the 9th floor to values of 0.20 cm in NS and 0.18 cm in EW direction. The roof displacement reached a maximum of 0.23 cm in NS and 0.21 cm in EW direction. Displacement amplification over the entire building height (i.e. from ground floor to roof level) increased by a factor of about 4. Displacements amplitudes at the 9th floor and the roof were found to be very similar in magnitude.

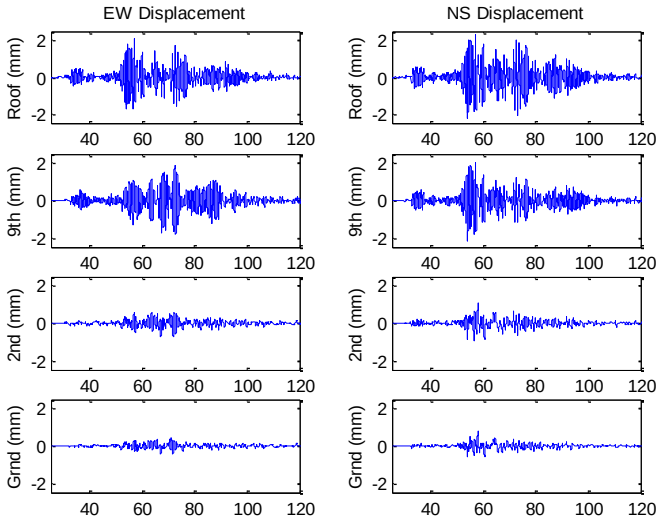


**Figure 3. 9.** Story displacements in EW and NS direction

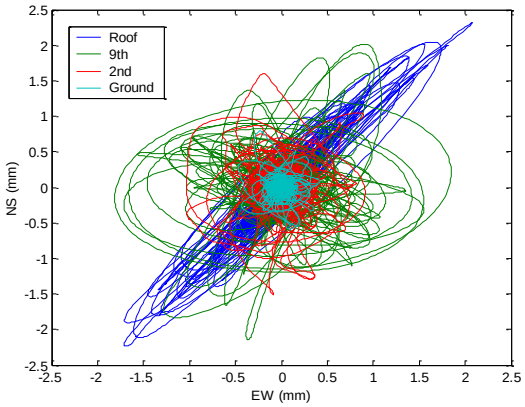


**Figure 3.10.** Particle motion *Building B*

Figure 3.10 shows particle motion as absolute displacements in the NS vs. EW direction measured for various levels in the building. It can be seen that floors 'Ground', 2 and 9 present patterns that move over the entire plane (uniformly circular). The roof level in turn shows a clear tendency to move along a diagonal path, which is consistent with the previous observation of the roof's EW and NS components shown in Figure 3.9. The roof sensor, which is eccentric relative to the other sensors, is influenced by a torsional mode given the synchrony between both displacement components. Figure 11 presents the transfer functions of the relative displacement response versus the normalized ground

acceleration determined at each instrumented floor. In order to smooth the observed response a Welsh procedure was implemented. From the analysis, the main frequency (*f*) and damping (β) parameters were determined to be f=1.09Hz and β=3.0% in NS direction, and *f* = 1.2Hz, β=2.2% in the EW direction. The largest amplitude of the relative displacement response occurred at a frequency of 1.09 Hz in the NS direction at the roof level.

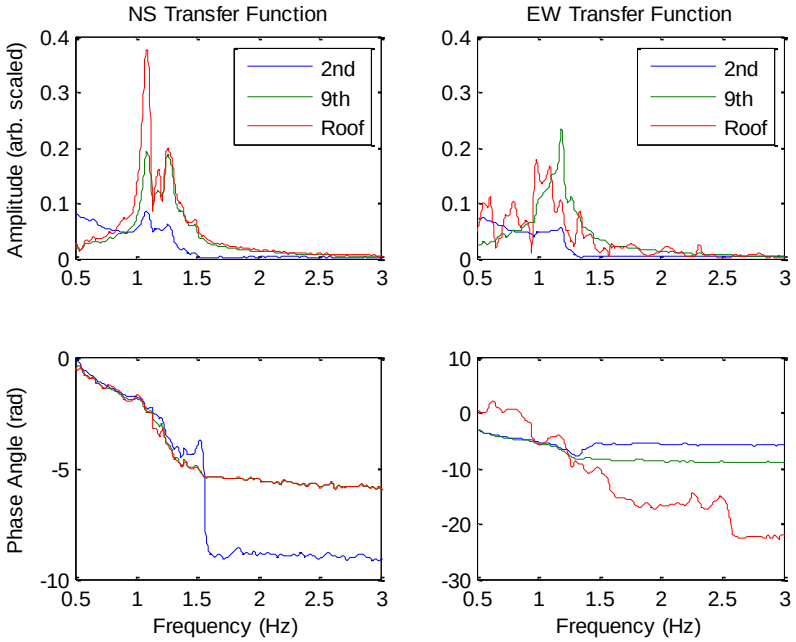


**Figure 3. 11** Transfer functions for *Building B*

The maximum absolute accelerations of selected floors were compared with pseudo spectral accelerations (PSA) determined for a single degree of freedom system (SDOF) using the measured building parameters (natural frequency and damping) that were observed in the corresponding direction (i.e., NS: f = 1.09Hz, β = 3.0%; EW: f = 1.2Hz, β = 2.2%). The results for both directions are presented in Figure 3.12a&b. A trend line (best fit analysis) is included to show the linear trend between the maximum floor accelerations and the intensity of the 22 aftershocks used for this analysis. Although, increases of PSA result in increases of maximum acceleration at different levels, the 2$^{nd}$ floor presents little correlation with PSA ($R^2$<0.4).

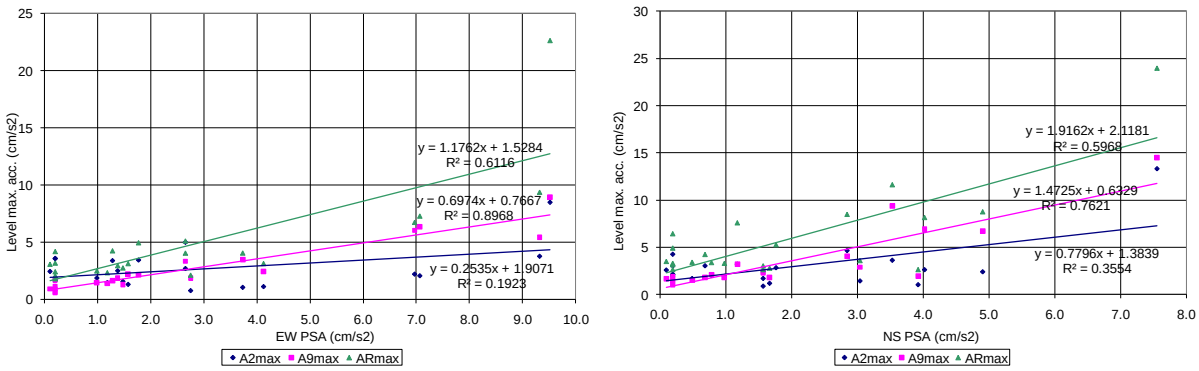


**Figure 3. 12a&b:** Comparison of measured floor accelerations and PSA analysis

Figure 3.13 shows a comparison of the maximum relative displacements of various floor levels with the results of the pseudo spectral analysis. Similarly to the previous analysis a linear best fit curve is also presented. Good correlation is observed between the displacement and PSA ($R^2$>0.8) for all levels of *Building B*. Additional studies were conducted for absolute displacements and showed consistent

results when compared against peak ground displacements (PGD). It can also be seen that close trends are obtained for the 9th and roof floors. All curves aim for zero displacement at zero PSA.

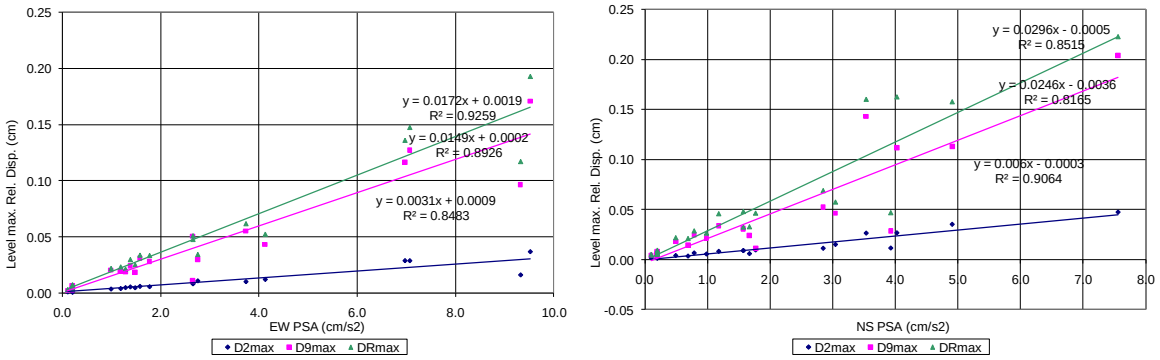


**Figure 3. 13** Comparison of relative floor displacements with peak ground displacements (PGD)

The instrumentation in *Building B* included the installation of linear voltage differential transducers (LVDTs) across a damaged shear wall on the first floor of the building. A photograph of the wall and the sensor instrumentation is shown in Figure 3.14. One pair of LVDTs was installed in diagonal configuration to enable the calculation of shear deformations during the aftershock. Another pair of vertical LVDTs was placed at both ends of the wall, spanning over the entire story height to determine the rotation due to flexural deformations. Since deformations are small, the diagonal sensors allowed for estimating the shear component of the first story lateral deformations in the wall plane. The flexural component was estimated by assuming a concentration of such deformation at wall base and that overall deformations in the wall are dominated by shear.

A time history of shear and flexure displacements during the March 25 aftershock is presented in Figure 3.15. The results indicate that the deformations are dominated by the shear component reaching about 0.2mm of lateral deformation, whereas the flexural component reaches about 0.04mm, which is only 20% of the shear component.

**Figure 3.14** Instrumentation of damaged wall in Building B.

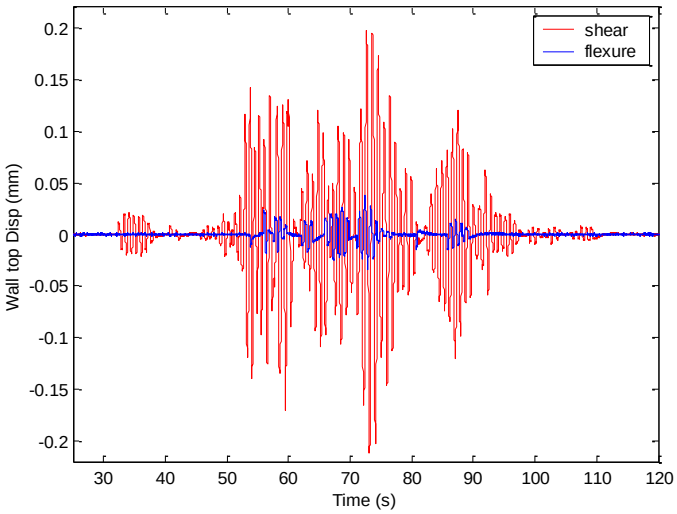


**Figure 3.15** Shear and flexural components of wall shear displacement

## SUMMARY AND CONCLUSIONS

Two reinforced concrete buildings were instrumented with accelerometers and LVDTs to record aftershock response data to determine seismic building parameters and enable future modelling studies. Both buildings were 10 story structures with different lateral force resisting systems, i.e. a

moment frame system and a shear wall system. Accelerations in both buildings increased by a factor of 2.5- 4 in EW or NS directions between ground and roof floors. First mode building frequencies were about 0.9-1.2 Hz with corresponding building periods of T = 0.83 - 1.1 sec. A strong sensitivity to torsional accelerations was observed in the damaged shear wall building. An instrumented reinforced concrete shear wall showed that shear displacements were stronger by a factor of 5 compared to measure flexural deformations during the aftershock. All data are stored at the NEES project warehouse and form a first initiative to create a public database for building response data to seismic events.

**AKCNOWLEDGEMENTS**

This instrumentation study was funded through an award granted by the National Science Foundation (NSF RAPID - CMMI 1040574, PI: John Wallace). Supplementary travel support was provided by the Earthquake Engineering Research Institute (EERI) as part of the 2010 Chile Earthquake reconnaissance efforts. The authors would like to acknowledge the Network for Earthquake Engineering Simulation (NEES) which provided the instrumentation and data acquisition equipment for the field study as part of the NEES-SHARED USE program. We would also like to acknowledge the help of a team consisting of local and international professionals and students without whom this process would not have been made possible at the speed and organizational management at which it was completed: Alberto Salamanca and Robert Nigbor (NEES@UCLA), Matias Chacom, Javier Encina and Joao Marques (Pontificia Universidad Cathólica de Chile), Marc Sereci (Digitexx) and Aditya Jain (ON Semiconductor).

**REFERENCES**

Earthquake Engineering Research Institute (EERI). (2010). "The $M_w$ 8.8 Chile Earthquake of February 27, 2010." *EERI Special Earthquake Report. June 2010*, <http://www.eeri.org/site/images/eeri_newsletter/2010_pdf/Chile10_insert.pdf> (May 2010).

International Building Code (2010). International Code Council, Whittier, CA

MATLAB (2010). MATLAB Version 7.10. Natick, Massachusetts: The Mathworks Inc., 2010